ARTICLE IN PRESS

Available online at www.sciencedirect.com

SCIENCE DIRECT

Journal of Solid State Chemistry 179 (2006) 877–883

JOURNAL OF SOLID STATE CHEMISTRY

www.elsevier.com/locate/jssc

Crystal structure and magnetic properties of $Co_2TeO_3Cl_2$ and $Co_2TeO_3Br_2$

Richard Becker[a,*], Helmuth Berger[b], Mats Johnsson[a], Mladen Prester[c], Zeljko Marohnic[c], Marko Miljak[c], Mirta Herak[c]

[a]*Department of Inorganic Chemistry, Stockholm University, S-106 91 Stockholm, Sweden*
[b]*Institut de Physique de la Matiere Complexe, Ecole Polytechnique Fédérale de Lausanne, CH-1015 Lausanne, Switzerland*
[c]*Institute of Physics, POB 304, HR-10000 Zagreb, Croatia*

Received 14 October 2005; received in revised form 1 December 2005; accepted 4 December 2005

We would like to dedicate this paper to Professor Francis Levy on the occasion of his 65th birthday

Abstract

The crystal structures of the two new synthetic compounds $Co_2TeO_3Cl_2$ and $Co_2TeO_3Br_2$ are described together with their magnetic properties. $Co_2TeO_3Cl_2$ crystallize in the monoclinic space group $P2_1/m$ with unit cell parameters $a = 5.0472(6)$ Å, $b = 6.6325(9)$ Å, $c = 8.3452(10)$ Å, $\beta = 105.43(1)^\circ$, $Z = 2$. $Co_2TeO_3Br_2$ crystallize in the orthorhombic space group $Pccn$ with unit cell parameters $a = 10.5180(7)$ Å, $b = 15.8629(9)$ Å, $c = 7.7732(5)$ Å, $Z = 8$. The crystal structures were solved from single crystal data, $R = 0.0328$ and 0.0412, respectively. Both compounds are layered with only weak interactions in between the layers. The compound $Co_2TeO_3Cl_2$ has $[CoO_4Cl_2]$ and $[CoO_3Cl_3]$ octahedra while $Co_2TeO_3Br_2$ has $[CoO_2Br_2]$ tetrahedra and $[CoO_4Br_2]$ octahedra. The Te(IV) atoms are tetrahedrally $[TeO_3E]$ coordinated in both compounds taking the $5s^2$ lone electron pair E into account. The magnetic properties of the compounds are characterized predominantly by long-range antiferromagnetic ordering below 30 K.

Keywords: Oxohalogenide; Stereochemically active lone electron pair; Layered crystal structure; Magnetic order; Antiferromagnetic

1. Introduction

Transition metal oxohalogenide compounds containing so-called lone-pair cations, e.g. Te^{4+}, Se^{4+}, Sb^{3+} and As^{3+}, having stereochemically active electron pairs has proved to be a family of compounds having a rich structure chemistry where there is a high probability to find novel low-dimensional arrangements of the transition metal cations [1–3]. In an oxohalogenide environment the late transition metal cations form bonds to both oxygen- and chlorine/bromine anions while lone-pair cations tend to form bonds only to oxygen anions. This chemical difference is utilized to reduce the dimensionality of the transition metal cation arrangement. Several novel oxohalogenide compounds with interesting magnetic properties have recently been synthesized, e.g. the compound $Cu_2Te_2O_5X_2(X = Cl, Br)$ where the weak coupling in between the Cu tetrahedra can be tuned by stoichiometry and pressure [1,4,5]. However, the family of Co^{2+} containing oxohalogenides including a lone-pair cation is surprisingly small. A search in the ICSD database for oxohalogenide compounds containing Co^{2+} and a lone-pair cation (Se^{4+}, Te^{4+}, As^{3+}, Sb^{3+}, Bi^{3+}) only revealed the following compounds: $Ba_2Co(SeO_3)_2Cl_2$ [6], $SmCo(SeO_3)_2Cl$ [7], $Co(HSeO_3)Cl \cdot 2(H_2O)$ [8], and $Co(HSeO_3)Cl \cdot 3(H_2O)$ [9].

The objective of this work was to replace non-magnetic Zn^{2+} in the zinc tellurium oxochloride $Zn_2TeO_3Cl_2$ [10] by magnetic Co^{2+}. The study resulted in two new compounds $Co_2TeO_3Cl_2$ and $Co_2TeO_3Br_2$. The bromide compound is isostructural with $Zn_2TeO_3Cl_2$ while the chloride compound exhibits a new crystal structure type. Magnetic susceptibilities of the novel compounds have been

*Corresponding author. Fax: +46 8 15 21 87.
E-mail address: richard@inorg.su.se (R. Becker).

0022-4596/$ - see front matter © 2005 Elsevier Inc. All rights reserved.
doi:10.1016/j.jssc.2005.12.007

measured by both dc- and ac-susceptibility techniques. A high-temperature Curie–Weiss law is compatible with the presence of antiferromagnetic correlations between the Co^{2+} magnetic moments.

2. Experimental

2.1. Synthesis and crystal growth

The new compounds $Co_2TeO_3Cl_2$ and $Co_2TeO_3Br_2$ were synthesized via chemical vapor transport reactions. The starting materials were CoO (Alfa Aesar 99.999%), TeO_2 (Acros 99%) and CoX_2 (X = Cl, Br) (Alfa Aesar 99.9%). It is possible to synthesize the compounds from stoichiometric molar ratios (1:1:1) of the starting materials, but the big single crystals used in this study were grown from the off-stoichiometric molar ratios $CoO:TeO_2:CoX_2 = 4:3:1$. The starting powders were mixed, grinded and compacted into pellets and placed in silica ampoules that were sealed after evacuation to 10^{-5} Torr. The ampoules were heated slowly to 550 °C in a horizontal electric furnace and held for 4 days followed by slow cooling by 50 °C/h to room temperature. The sintered pellets were blue and polyphasic and their phase composition were not analyzed. Single crystals of the new compounds were prepared by chemical vapor transport from the sintered pellets as detailed below.

For $Co_2TeO_3Cl_2$, a portion (about 5–10 g) of powder from crunched pellets of the primary reaction products was enclosed in evacuated (10^{-5} Torr) and sealed silica ampoules, along with electronic grade HCl as transporting agent. The ampoules were then placed in two-zone gradient furnaces. Charge and growth-zone temperatures were 600 and 450 °C, respectively. After few weeks, thin purple transparent needle-like platelets with a typical size of $10 \times 2 \times 0.02\,mm^{-3}$ of $Co_2TeO_3Cl_2$ had grown in the colder part of the ampoule.

For $Co_2TeO_3Br_2$ a portion of the prepared material was placed in a silica tube and subsequently evacuated. Electronic grade HBr, to which a very small amount of electronic grade HCl has been added, was used as the transport agent. The ampoule was placed in a two-zone gradient furnace, where charge and growth-zone temperatures were 650 and 400 °C, respectively. After 2 months, the formation of crystals was observed in the ampoule.

Single crystals of $Co_2TeO_3Br_2$ with different morphology were found in the hot and in the cold part of the ampoule. Blue needles with a typical size of $10 \times 2 \times 0.04\,mm^{-3}$ had grown in the hot part and light blue platelets with a typical size of $6 \times 6 \times 0.02\,mm^{-3}$ had grown in the colder part of the ampoule.

The synthesized crystals were characterized in a scanning electron microscope (SEM, JEOL 820) with an energy-dispersive spectrometer (EDS, LINK AN10000) confirming the presence and stoichiometry of Co, Te, Br, and Cl.

2.2. Crystal structure determination

Single-crystal X-ray data were collected on an Oxford Diffraction Xcalibur3 diffractometer using graphite-monochromatized Mo$K\alpha$ radiation, $\lambda = 0.71073$ Å. The intensities of the reflections were integrated using the software supplied by the manufacturer. Numerical absorption correction was performed with the programs X-red [11] and X-shape [12]. The crystal structures were solved by direct methods using the program SHELXS97 [13] and refined by full matrix least squares on F^2 using the program SHELXL97 [14]. All atoms are refined with anisotropic displacement parameters. Experimental parameters, atomic coordinates and selected interatomic distances for $Co_2TeO_3Cl_2$ and $Co_2TeO_3Br_2$ are reported in Tables 1, 2a,b and 3a,b respectively.

2.3. Magnetic susceptibility measurements

High-resolution magnetic ac susceptibility was measured by a commercial CryoBIND system. Measuring amplitude of the applied ac magnetic fields was relatively small (of the

Table 1
Crystal data for $Co_2TeO_3Cl_2$ and $Co_2TeO_3Br_2$

Empirical formula	$Co_2TeO_3Cl_2$	$Co_2TeO_3Br_2$
Formula weight	364.36	453.28
Temperature	293(2) K	293(2) K
Wavelength	0.70930	0.70930
Crystal system	Monoclinic	Orthorhombic
Space group	$P2_1/m$	$Pccn$
Unit cell dimensions	$a = 5.0472(6)$ Å $b = 6.6325(9)$ Å $c = 8.3452(10)$ Å $\beta = 105.43(1)^\circ$	$a = 10.5180(7)$ Å $b = 15.8629(9)$ Å $c = 7.7732(5)$ Å
Volume (Å^3)	269.29(6)	1296.93(14)
Z	2	8
Density (calculated)	4.494 g cm^{-3}	4.643 g cm^{-3}
Absorption coefficient	12.354 mm^{-1}	21.761 mm^{-1}
Absorption correction	Numerical	Numerical
$F(000)$	328	1600
Crystal color	Purple	Blue
Crystal habit	Think flakes	Thin flakes
Crystal size (mm^3)	$0.2 \times 0.055 \times 0.010$	$0.120 \times 0.055 \times 0.010$
θ range for data collection	3.97–31.91°	4.14–30.43°
Index ranges	$-7 \leqslant h \leqslant 7$ $-9 \leqslant k \leqslant 9$ $-12 \leqslant l \leqslant 12$	$-15 \leqslant h \leqslant 15$ $-22 \leqslant k \leqslant 22$ $-11 \leqslant l \leqslant 11$
Reflections collected	5519	1971
Independent reflections	1000[R(int) = 0.0648]	1591[R(int) = 0.0986]
Completeness to θ = max°	99%	99%
Refinement method	Full-matrix least squares on F^2	Full-matrix least squares on F^2
Data/restraints/parameters	1000/0/47	1971/0/73
Goodness-of-fit on F^2	1.021	1.078
Final R indices [$I > 2\theta(I)$]	$R_1 = 0.0328$ w$R_2 = 0.0806$	$R_1 = 0.0412$ w$R_2 = 0.1004$
R indices (all data)	$R_1 = 0.0389$ w$R_2 = 0.0825$	$R_1 = 0.0604$ w$R_2 = 0.1092$
Largest diff. peak and hole	2.035 and –1.902 (e Å^{-3})	1.584 and –1.996 (e Å^{-3})

Table 2
Atomic coordinates and equivalent isotropic displacement parameters

Atom	Wyck.	X	y	Z	U_{eq}[a] (Å^2)
(a) $Co_2TeO_3Cl_2$					
Te	2*e*	0.5930(1)	$\frac{1}{4}$	0.24668(4)	0.0128(2)
Co(1)	2*a*	0	0	0	0.0142(2)
Co(2)	2*e*	0.2452(2)	$\frac{1}{4}$	0.7752(1)	0.0168(2)
Cl(1)	2*e*	0.7464(2)	$\frac{1}{4}$	0.7913(2)	0.0173(3)
Cl(2)	2*e*	0.1626(3)	$\frac{1}{4}$	0.4921(2)	0.0311(4)
O(1)	4*f*	0.7568(6)	0.0390(4)	0.1596(3)	0.0158(6)
O(2)	2*e*	0.2531(8)	$\frac{1}{4}$	0.0735(5)	0.0167(8)
(b) $Co_2TeO_3Br_2$					
Te	8*e*	0.5263(1)	0.4025(1)	0.2115(1)	0.0190(2)
Co(1)	8*e*	0.4969(1)	0.6025(1)	0.3473(1)	0.0232(2)
Co(2)	8*e*	0.7700(1)	0.4620(1)	0.3943(1)	0.0224(2)
Br(1)	8*e*	0.7115(1)	0.6212(1)	0.4480(1)	0.0325(2)
Br(2)	8*e*	0.4074(1)	0.7048(1)	0.1570(1)	0.0387(2)
O(1)	8*e*	0.6875(4)	0.4398(3)	0.1427(7)	0.0234(1)
O(2)	8*e*	0.4461(4)	0.5091(3)	0.1945(7)	0.0231(1)
O(3)	8*e*	0.5872(5)	0.4187(3)	0.4361(7)	0.0245(1)

[a] U_{eq} is defined as one-third of the trace of the orthogonalized U tensor.

Table 3a
Selected bond lengths (Å) and bond angles (°) for $Co_2TeO_3Cl_2$

Te–Cl(2)^{ii}	3.054(2)	O(1)^{iii}–Co(1)–O(2)	82.3(1)
Te–O(1)	1.869(3)	O(1)^{iv}–Co(1)–O(2)^{v}	82.3(1)
Te–O(1)^{i}	1.869(3)	O(1)^{iv}–Co(1)–Cl(1)^{vi}	85.13(8)
Te–O(2)	1.926(4)	O(1)^{iv}–Co(1)–Cl(1)^{vii}	94.87(8)
Co(1)–Cl(1)^{vi}	2.497(1)	O(1)^{iv}–Co(1)–O(2)	97.7(1)
Co(1)–Cl(1)^{vii}	2.497(1)	O(1)^{iii}–Co(1)–O(2)^{v}	97.7(1)
Co(1)–O(1)^{iii}	2.053(3)	O(2)–Co(1)–Cl(1)^{vi}	99.37(9)
Co(1)–O(1)^{iv}	2.053(3)	O(2)–Co(1)–Cl(1)^{vii}	80.63(9)
Co(1)–O(2)	2.084(2)	O(2)^{v}–Co(1)–Cl(1)^{vi}	80.63(9)
Co(1)–O(2)^{v}	2.084(2)	O(2)^{v}–Co(1)–Cl(1)^{vii}	99.37(9)
Co(2)–Cl(1)	2.498(1)	O(2)^{v}–Co(1)–O(2)	180.0(3)
Co(2)–Cl(1)^{iv}	2.556(1)	Cl(1)–Co(2)–Cl(1)^{iv}	174.12(7)
Co(2)–Cl(2)	2.287(2)	Cl(2)–Co(2)–Cl(1)	87.66(6)
Co(2)–O(1)^{vi}	1.993(3)	Cl(2)–Co(2)–Cl(1)^{iv}	98.21(6)
Co(2)–O(1)^{viii}	1.993(3)	Cl(2)–Co(2)–O(2)^{ix}	170.8(1)
Co(2)–O(2)^{ix}	2.479(4)	O(1)^{vi}–Co(2)–Cl(1)	93.67(8)
		O(1)^{vi}–Co(2)–Cl(1)^{iv}	84.78(8)
O(1)–Te–O(1)^{i}	97.0(2)	O(1)^{vi}–Co(2)–Cl(2)	105.62(9)
O(1)–Te–O(2)	96.1(1)	O(1)^{vi}–Co(2)–O(2)^{ix}	74.08(8)
O(1)–Te–Cl(2)^{ii}	79.97(9)	O(1)^{viii}–Co(2)–Cl(1)	93.67(8)
O(1)^{i}–Te–O(2)	96.1(1)	O(1)^{viii}–Co(2)–Cl(1)^{iv}	84.78(8)
O(1)^{i}–Te–Cl(2)^{ii}	79.97(9)	O(1)^{viii}–Co(2)–Cl(2)	105.62(9)
O(2)–Te–Cl(2)^{ii}	174.0(1)	O(1)^{viii}–Co(2)–O(1)^{vi}	148.1(2)
Cl(1)^{vi}–Co(1)–Cl(1)^{vii}	180.00(5)	O(1)^{viii}–Co(2)–O(2)^{ix}	74.08(8)
O(1)^{iii}–Co(1)–Cl(1)^{vi}	94.87(8)	O(2)^{ix}–Co(2)–Cl(1)	101.6(1)
O(1)^{iii}–Co(1)–Cl(1)^{vii}	85.13(8)	O(2)^{ix}–Co(2)–Cl(1)^{iv}	72.56(9)
O(1)^{iii}–Co(1)–O(1)^{iv}	180.0(1)		

Note: Symmetry transformations used to generate equivalent atoms: (i) x, $0.5-y$, z; (ii) $1+x$, y, z; (iii) $1-x$, $-y$, $-z$; (iv) $-1+x$, y, z; (v) $-x$, $-y$, $-z$; (vi) $1-x$, $-y$, $1-z$; (vii) $-1+x$, y, $-1+z$; (viii) $1-x$, $0.5+y$, $1-z$; (ix) x, y, $1+z$.

order of few Oersteds), representing an important advantage in studies of any kind of spontaneous magnetic ordering. Magnetic dc susceptibility was measured by the Faraday balance method in the measuring field of 5 kG.

Table 3b
Selected bond lengths (Å) and bond angles (°) for $Co_2TeO_3Br_2$

Te–O(1)	1.873(5)	O(2)–Co(1)–Br(2)	91.8(2)
Te–O(2)	1.895(5)	O(3)^{i}–Co(1)–Br(1)	99.6(2)
Te–O(3)	1.877(5)	O(2)–Co(1)–Br(1)	122.8(2)
Co(1)–Br(1)	2.407(1)	Br(2)–Co(1)–Br(1)	119.16(5)
Co(1)–Br(2)	2.389(1)	Br(2)^{iii}–Co(2)–Br(1)	165.52(4)
Co(1)–O(2)	1.973(5)	Br(2)^{iii}–Co(2)–O(1)	86.1(1)
Co(1)–O(3)^{i}	1.931(5)	Br(2)^{iii}–Co(2)–O(1)^{ii}	82.6(1)
Co(2)–Br(1)	2.634(1)	Br(2)^{iii}–Co(2)–O(2)^{iii}	73.8(1)
Co(2)–Br(2)^{iii}	3.037(1)	Br(2)^{iii}–Co(2)–O(3)	99.8(2)
Co(2)–O(1)	2.173(5)	O(1)–Co(2)–Br(1)	101.6(1)
Co(2)–O(1)^{ii}	2.011(5)	O(1)^{ii}–Co(2)–Br(1)	93.9(2)
Co(2)–O(2)^{iii}	2.020(5)	O(1)^{ii}–Co(2)–O(1)	157.5(2)
Co(2)–O(3)	2.078(5)	O(1)^{ii}–Co(2)–O(2)^{iii}	99.8(2)
		O(1)^{ii}–Co(2)–O(3)	89.7(2)
O(1)–Te–O(3)	85.1(2)	O(2)^{iii}–Co(2)–Br(1)	93.1(1)
O(1)–Te–O(2)	95.8(2)	O(2)^{iii}–Co(2)–O(1)	95.6(2)
O(3)–Te–O(2)	95.4(2)	O(2)^{iii}–Co(2)–O(3)	167.7(2)
O(3)^{i}–Co(1)–O(2)	105.6(2)	O(3)–Co(2)–Br(1)	94.1(2)
O(3)^{i}–Co(1)–Br(2)	118.5(2)	O(3)–Co(2)–O(1)	73.2(2)

Note: Symmetry transformations used to generate equivalent atoms: (i) $1-x$, $1-y$, $1-z$; (ii) $1.5-x$, y, $0.5+z$; (iii) $0.5+x$, $1-y$, $0.5-z$.

3. Results and discussion

3.1. Crystal structure of $Co_2TeO_3Cl_2$

The purple $Co_2TeO_3Cl_2$ single crystals are non-hygroscopic, and crystallize in the monoclinic system, space group $P2_1/m$. There are two crystallographically different Co atoms that both have the oxidation state (+II) which has been confirmed by bond valence sum calculations [15,16]. The Co(1) atom is coordinated by four oxygen anions, two at the distance 2.053(3) Å and two at 2.084(2) Å, in a square plane and further to two chlorine atoms both at 2.497(1) Å completing a $[CoO_4Cl_2]$ octahedron. The Co(2) atom is coordinated by three oxygen atoms, two at the distance 1.993(3) Å and one at 2.479(4) Å, and to three chlorine atoms at distances in the range 2.287(2)–2.556(1) Å, forming the unusual distorted $[CoO_3Cl_3]$ octahedron, see Table 3a for more details on bond lengths and angles. The Te atom has the oxidation state (+IV) and has a typical one-sided three-fold coordination due to the presence of the $5s^2$ stereochemically active lone pair (designated E). The coordination polyhedron of the Te atom is that of a $[TeO_3E]$ tetrahedron with Te–O distances in the range 1.869(3)–1.926(4) Å. A fourth ligand, a Cl^- ion, is observed at a Te–Cl(2) distance of 3.054(2) Å which would complete a trigonal bi-pyramidal $[TeO_3ClE]$ coordination. Bond valence sum calculations using the most recent data reported by Brown [15] and bond definitions according to Brown [16] implies that the maximum Te–Cl distance to be considered as a primary bonding distance is 3.05 Å and thus this Cl^- ion is just on the border of the primary coordination sphere and can thus be considered both as bonded and non-bonded. The presence of a fourth ligand (which typically is a fourth

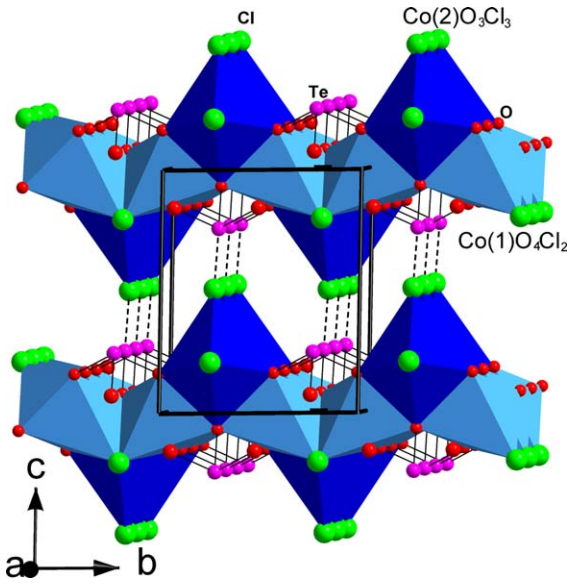

Fig. 1. The crystal structure of $Co_2TeO_3Cl_2$ is layered and the layers are kept together via a weak Te–Cl(2) interaction (dotted).

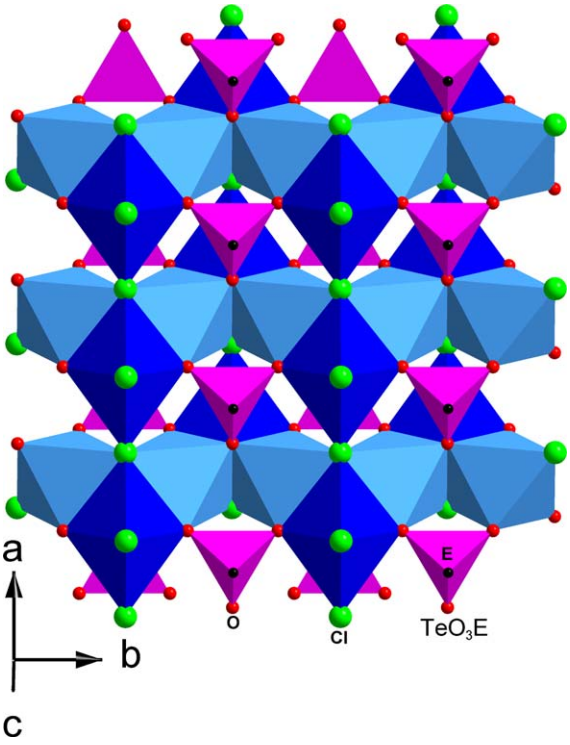

Fig. 2. The chains of Co-polyhedra are linked via Cl^- ions. Also the $[TeO_3E]$ polyhedra help to connect the chains to build up a layer in $Co_2TeO_3Cl_2$.

oxygen ion) around Te^{4+} positioned just at the, according to Brown, verge of what can be considered inside the primary coordination sphere, e.g. 2.66 Å for Te^{4+}–O^{2-} bonds, has been observed in several compounds, e.g. $Cu_2Te_2O_5Cl_2$ and $Ni_5(TeO_3)_4Cl_2$ which have a fourth Te–O distance at 2.545 and 2.675 Å, respectively [1,2].

The three building blocks $[Co(1)O_4Cl_2]$, $[Co(2)O_3Cl_3]$ and $[TeO_3E]$ are arranged to form layers in the structure. The layers are only connected via the weak Te–Cl(2) interaction discussed above (see Fig. 1). In each layer the $[Co(1)O_4Cl_2]$ octahedra form chains along [010] by edge sharing. The $[CoO_3Cl_3]$ octahedrons are then connected to the $[CoO_4Cl_2]$ chains so that each $[CoO_3Cl_3]$ octahedron shares common faces with two different $[CoO_4Cl_2]$ octahedrons. The chains of Co-octahedra are connected to adjacent chains both via corner sharing at the Cl(1) atoms and also by corner sharing at the oxygen atoms with the $[TeO_3E]$ tetrahedra (see Fig. 2). The layers have no net charge and the Cl(2) atoms and the stereochemically active lone pairs of Te^{4+} can be seen protruding out from these layers. The shortest Co–Co distance between two layers is ~5.6 Å.

3.2. Crystal structure of $Co_2TeO_3Br_2$

The blue $Co_2TeO_3Br_2$ single crystals are non-hygroscopic, and crystallize in the orthorhombic system, space group *Pccn*. The new compound is isostructural with the mineral sophiite, $Zn_2SeO_3Cl_2$ [17], and the synthetic compounds $Zn_2TeO_3Cl_2$ and $CuZnTeO_3Cl_2$ [10,18]. There are two crystallographically different Co positions. The Co(1) atom is coordinated by two oxygen atoms at the distances 1.931(5) and 1.973(5) Å, and by two bromine atoms at 2.389(1) and 2.407(1) Å, respectively, to form a distorted $[CoO_2Br_2]$ tetrahedron. The Co(2) atom on the other hand has an distorted octahedral $[CoO_4Br_2]$ coordination with Co–O distances in the range 2.011(5)–2.173(5) Å and Co–Br distances at 2.634(1) and 3.037(1) Å. The Te ion has the oxidation state (+IV) and shows the classical $[TeO_3E]$ tetrahedral coordination with an additional oxygen atom far outside the coordination sphere.

The polyhedra $[Co(1)O_2Br_2]$, $[Co(2)O_4Br_2]$, and $[TeO_3E]$ are connected to form layers of no net charge in the crystal structure (see Fig. 3). In the layers there are chains of corner-sharing $[Co(2)O_4Br_2]$ octahedra running along the [001] axis. These Co-chains are connected to the neighboring chains via edge and corner sharing to the $[Co(1)O_2Br_2]$ and the $[TeO_3E]$ tetrahedrons (see Fig. 4). The Br^- ions and the lone pairs of the Te^{4+} ions separate the layers from each other so that there are only weak van der Waals interactions in between adjacent layers (see Fig. 3).

EDS data on crystals of $Co_2TeO_3Br_2$ implies that the Br positions are in fact occupied by a small (~5%) amount of Cl. A structural refinement where this was allowed gave the resulting formula to be $Co_2TeO_3Br_{1.88}Cl_{0.12}$ (i.e. ~6% Cl). This will lower the *r*-value of the structure refinement somewhat but not significantly. The small amount of Cl present can be explained by the HCl used in combination with HBr as a transporting agent during the synthesis.

3.3. Magnetic properties

Magnetic susceptibilities of $Co_2TeO_3Cl_2$ and $Co_2TeO_3Br_2$ samples have been measured by both dc- and

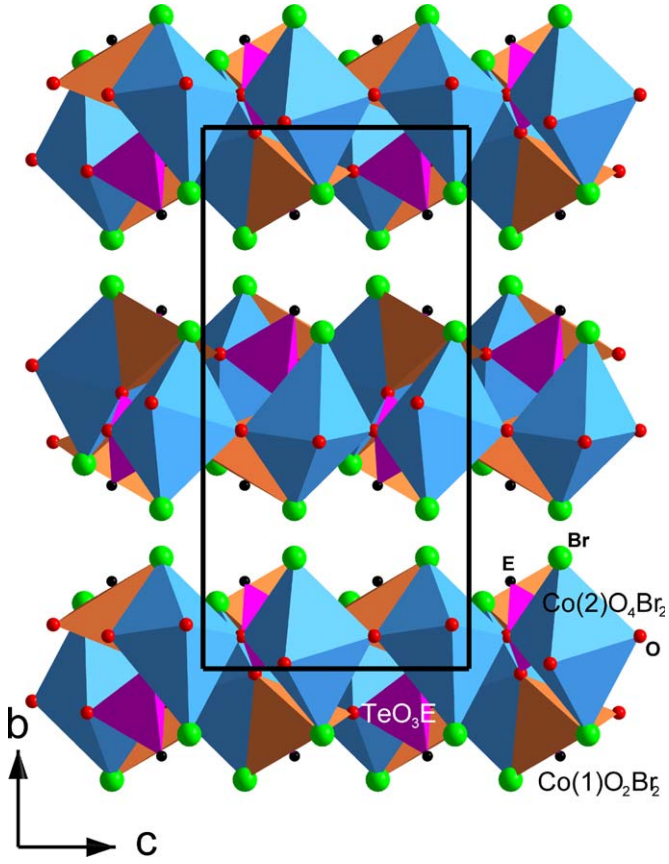

Fig. 3. The layered crystal structure of $Co_2TeO_3Br_2$. Only weak van der Waal bonds connect the layers.

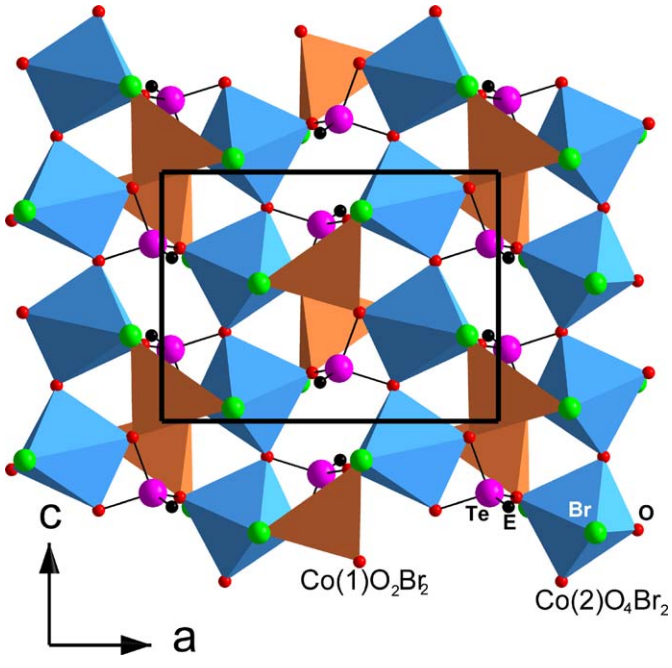

Fig. 4. Layer of $Co_2TeO_3Br_2$ consisting of $[CoO_4Br_2]$ octahedrons connected by the $[CoO_2Br_2]$ tetrahedrons and the $[TeO_3E]$ groups.

ac-susceptibility techniques. At high temperatures the dc-susceptibility of the powdered single crystals of both compounds can be well described in a broad temperature

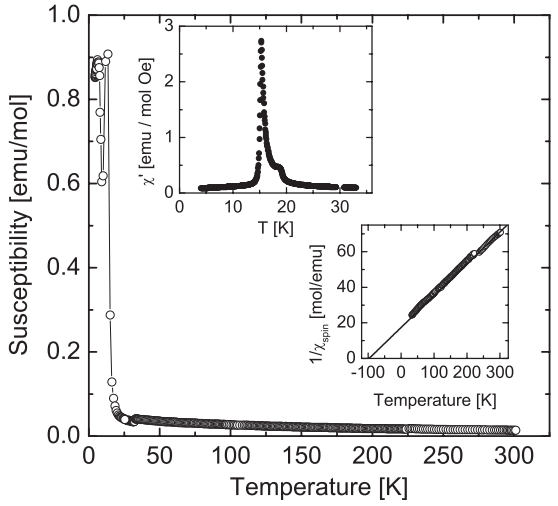

Fig. 5. The dc susceptibility of $Co_2TeO_3Cl_2$ (main panel). Parameters of the Curie–Weiss fit (inset in the right corner) are: Curie constant $C = 5.63\,\text{emu K/mol}$ ($g \approx 2.45$), Weiss temperature $\theta_{CW} = -97\,\text{K}$. The top inset shows ac susceptibility with measuring field 3.5 Oe at the frequency of 430 Hz. Two ordering events, at 18.5 and 15 K, are clearly indicated.

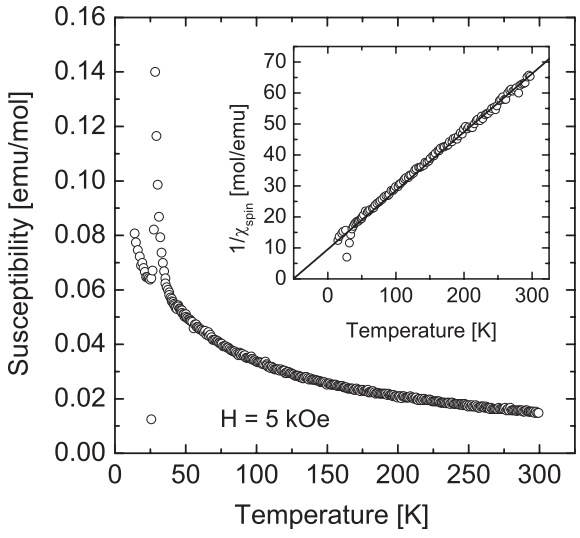

Fig. 6. The dc susceptibility of $Co_2TeO_3Br_2$. Parameters of the Curie–Weiss fit (inset) are: Curie constant $C = 5.21\,\text{emu K/mol}$ ($g \approx 2.34$), Weiss temperature $\theta_{CW} = -46\,\text{K}$.

range 50–330 K by a Curie–Weiss type of temperature dependence, $1/\chi = (T - \theta_{CW})/C$ (see Figs. 5 and 6). At low temperatures magnetic ordering sets in. In the higher temperature regime Curie–Weiss linear data fit give Curie constants of $C = 5.63$ and 5.21 emu K/mol for $Co_2TeO_3Cl_2$ and $Co_2TeO_3Br_2$, respectively. The related g-factor values can be approximated by $g \approx 2.4$. These numbers are in full agreement with literature data for Co^{2+}, $S = 3/2$, spin state. The Weiss constant θ_{CW}, is systematically negative in sign revealing antiferromagnetic spin correlations.

Spontaneous magnetic ordering is best studied in small measuring fields. The magnetic ordering temperature ranges of the compounds have been studied by

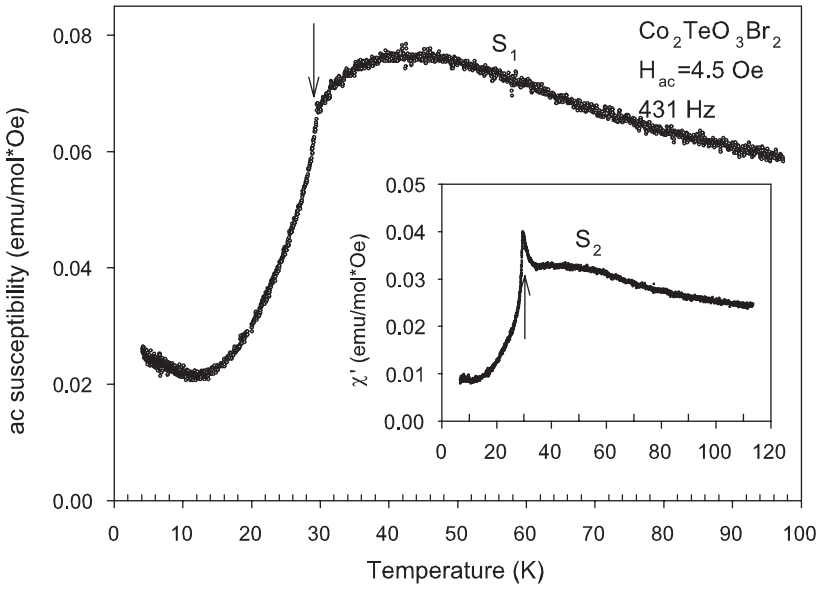

Fig. 7. The ac susceptibility of $Co_2TeO_3Br_2$ from two samples from different batches (S_1 and S_2) illustrating the sample dependence. Long-range magnetic order (arrow) sets-in at $T_N = 29$ K. There is a big error bar (not shown) in absolute susceptibility value introduced by small sample mass (at the order of 500 μg) and weighing error.

high-resolution ac susceptibility technique, employing measuring field of the order of 1 Oe (see Fig. 7) and inset in Fig. 5. In $Co_2TeO_3Cl_2$ magnetic ordering takes place at about 15–20 K. Actually, there is a sequence of at least two different ordering events. The shoulder at $T_{c1} = 18.5$ K, see the top inset to Fig. 5, is presumably related to ordering of antiferromagnetic nature while the pronounced peak at $T_{c2} = 15$ K involves, due to its intensity, some sort of ferromagnetic spin ordering or reorientations/alignments. We note that the relative height of the ferromagnetic peak depends on the applied field. In dc susceptibility studies of zero-field-cooled samples a strong nonlinearity of magnetization in increasing magnetic field has been observed. These observations are reminiscent of the behavior of metamagnets.

In $Co_2TeO_3Br_2$ there is $3d$ magnetic ordering at $T_N = 29$ K (see Fig. 7). The susceptibility behavior in the transition range is indicative of antiferromagnetic ordering, again consistent with antiferromagnetic correlations above T_N. Similarly as in the case of $Co_2TeO_3Cl_2$ there is some sample-batch dependence responsible for sample-specific susceptibility features shown in the inset to Fig. 7. Quite generally, the sample dependence of both the Br- and the Cl-compound might be a consequence of magnetically ordered planes playing the role of a magnetic structure building block: the latter sort of sample dependence is known to characterize, e.g., the intercalates. In the particular case of the Br-compound the mentioned deviations from the bromine stoichiometry can naturally be ascribed to underlay the sample dependence. However, for better understanding of the precise type of magnetic ordering/spin reorientations scheme one needs an insight into the presently unknown magnetic structure of the compounds. Owing to the relatively complex crystal structures, featuring two crystallographically different Co sites, modeling the magnetic structures is rather demanding and may be a subject for a separate study.

4. Conclusions

Relatively large single crystals of the new layered compounds $Co_2TeO_3Cl_2$ and $Co_2TeO_3Br_2$ have been synthesized in sealed silica tubes from the off stoichiometric molar ratios of $CoO:CoX_2:TeO_2$ (X = Cl, Br) 4:1:3 with HCl and HBr added, respectively, as transporting agents. The compounds have been found to have different crystal structures. $Co_2TeO_3Cl_2$ crystallize in the centrosymmetric monoclinic space group $P2_1/m$ while $Co_2TeO_3Br_2$ crystallize in the centrosymmetric orthorhombic space group $Pccn$. The compounds are layered, the layers have no net charge and there are only weak interactions in between the layers. $Co_2TeO_3Br_2$ is iso-structural with the mineral $Zn_2SeO_3Cl_2$ and the synthetic compounds $Zn_2TeO_3Cl_2$ and $ZnCuTeO_3Cl_2$ while $Co_2TeO_3Cl_2$ show a new crystal structure type. One may speculate that also the compounds $CoZnTeO_3X_2$ and $CoZnSeO_3X_2$ (X = Cl, Br) may exist. As Co^{2+} and Zn^{2+} both can take tetrahedral and octahedral coordination any such compounds may show a wider solid solution range than the Cu/Zn solid solutions.

At high temperatures magnetic susceptibility follows the Curie–Weiss behavior, characterized by negative Weiss constants ($\theta_{CW} = -97$ and –46 K for $Co_2TeO_3Cl_2$ and $Co_2TeO_3Br_2$, respectively). In the ground state the compounds are magnetically ordered. The results of ac- and dc-susceptibility measurements are consistent with

long-range antiferromagnetic order. For the $Co_2TeO_3Cl_2$ compound there is, however, a clear evidence of a ferromagnetic component in the sequence of ordering events indicating the complexity of magnetic order stabilized at low temperatures.

Acknowledgments

This work has in part been carried out with financial support from the Swedish Research Council. The work in Lausanne was supported by the Swiss National Science Foundation (SNSF) and by the MaNEP while the work in Zagreb was supported by the resources of the SNSF-SCOPES project. We are grateful to Prof. D. Pavuna for stimulating comments and discussions.

Supplementary material has been sent to Fachinformationzentrum Karlsruhe, Abt. PROKA, 76344 Eggenstein-Leopoldshafen, Germany (fax: +49-7247-808-666; E-mail: crysdata@fiz-karlsruhe.de), and can be obtained on quoting the deposit numbers CSD-415798 for $Co_2TeO_3Cl_2$ and CSD-415797 for $Co_2TeO_3Br_2$.

References

[1] M. Johnsson, K.W. Törnroos, F. Mila, P. Millet, Chem. Mater. 12 (2000) 2853–2857.
[2] M. Johnsson, K.W. Törnroos, P. Lemmens, P. Millet, Chem. Mater. 15 (2003) 68–73.
[3] R. Becker, M. Johnsson, R. Kremer, P. Lemmens, J. Solid State Chem. 178 (2005) 2024–2029.
[4] P. Lemmens, K.Y. Choi, G. Günterodt, M. Johnsson, P. Millet, F. Mila, R. Valenti, C. Gros, W. Brenig, Physica B 329–333 (2003) 1049–1050.
[5] J. Kreitlow, S. Süllow, D. Menzel, J. Schoenes, P. Lemmens, M. Johnsson, J. Magn. Magn. Mater. 290–291 (2005) 959–961.
[6] M.G. Johnston, W.T.A. Harrison, Acta Cryst. E 58 (2002) 49–51.
[7] M.S. Wickleder, M. Ben Hamida, Z. Anorg. Allg. Chem. 629 (2003) 556–562.
[8] M.G. Johnston, W.T.A. Harrison, Acta Cryst. E 59 (2003) 62–64.
[9] M.G. Johnston, W.T.A. Harrison, Z. Anorg. Allg. Chem. 626 (2000) 2487–2490.
[10] M. Johnsson, K.W. Törnroos, Acta Cryst. C 59 (2003) i53–i54.
[11] X-RED, Version 1.22, STOE & Cie GmbH, Darmstadt, Germany, 2001.
[12] X-SHAPE revision 1.06, STOE & Cie GmbH, Darmstadt, Germany, 1999.
[13] G.-M. Sheldrick, SHELXS-97—Program for the Solution of Crystal Structures, Göttingen, 1997.
[14] G.-M. Sheldrick, SHELXL-97—Program for the Refinement of Crystal Structures, Göttingen, 1997.
[15] I.D. Brown, Bond valence sum parameters, http://www.ccp14.ac.uk/ccp/web–mirrors/i_d_brown/bond_valence_param/.
[16] I.D. Brown, The Chemical Bond in Inorganic Chemistry: The Bond Valence Model, Oxford University Press, New York, 2002.
[17] T.F. Semenova, I.V. Rozhdestvenskaya, S.K. Filatov, L.P. Vergasova, Mineral. Mag. 56 (1992) 241–245.
[18] M. Johnsson, K.W. Törnroos, Solid State Sci. 5 (2003) 263–266.